NATIONAL ADVISORY COMMITTEE FOR AERONAUTICS

TECHNICAL NOTE 2237

CORRELATIONS OF HEAT-TRANSFER DATA AND OF FRICTION DATA FOR INTERRUPTED PLANE FINS STAGGERED IN SUCCESSIVE ROWS

By S. V. Manson

Lewis Flight Propulsion Laboratory
Cleveland, Ohio

Washington
December 1950

NATIONAL ADVISORY COMMITTEE FOR AERONAUTICS

TECHNICAL NOTE 2237

CORRELATIONS OF HEAT-TRANSFER DATA AND OF FRICTION DATA FOR INTERRUPTED PLANE FINS STAGGERED IN SUCCESSIVE ROWS

By S. V. Manson

SUMMARY

The available heat-transfer and friction data on plane fin surfaces that are interrupted and staggered in successive rows in the fluid-flow direction were separately correlated. The data presented were taken from five reference reports and cover wide ranges of flow Reynolds number, passage hydraulic diameter, fin transverse spacing, fin length in the fluid-flow direction, fin thickness, and various stagger arrangements of the fins.

A single heat-transfer correlation equation was obtained that satisfactorily represents the heat-transfer data over the entire range of conditions investigated. The friction data required separate correlation equations above and below the transition Reynolds number of 3500, based on the fin-passage hydraulic diameter. The bulk of the friction data available satisfactorily correlated.

INTRODUCTION

In fluid flow along a surface, high heat-transfer coefficients prevail at the initial portions of the surface (entrance region) where the fluid boundary layer is not yet fully developed. This fact can be used to advantage for finned heat-exchange surfaces by interrupting the fins. Experiments with interrupted fins have been performed by various investigators and experimental heat-transfer and friction data for such surfaces are reported in references 1 to 5.

Interrupted plane fins staggered in successive rows, as shown in references 1 to 5, combine high heat-transfer coefficients with friction factors that are lower than those obtained for nonplane fins (for example, pin fins or waved surfaces). Equations for predicting the performance of interrupted plane fins for use in heat-exchanger design would thus be desirable.

In reference 1, a good correlation based on the theoretical predictions of Blasius is presented for the heat-transfer data reported therein; however, not all the factors pertinent to the heat-transfer process were investigated. The friction data reported were not satisfactorily correlated on the basis predicted by Blasius and no effort was made to obtain a satisfactory correlation.

Because no attempt to correlate either the heat-transfer or the friction data available from the various independent investigators has been previously reported, correlations of the data of references 1 to 5 were made at the NACA Lewis laboratory and are presented herein.

SYMBOLS

The following symbols are used in this report:

A	cross-sectional area available for fluid flow, (sq ft)
c_p	specific heat of fluid at constant pressure, (Btu/(lb)($^\circ$F))
d_h	hydraulic diameter of fin passage, $4A/P_w$, (ft except where specified as in.)
F_1, F_2	functions
f	friction factor, $(\Delta p/(\rho v^2/2g)(4l/d_h))$
G	mass velocity (weight flow per unit cross-sectional area), (lb/(sec)(sq ft))
g	acceleration due to gravity, (32.2 ft/sec^2)
h	heat-transfer coefficient, (Btu/(sec)(sq ft)($^\circ$F))
k	thermal conductivity, (Btu/(sec)(ft)($^\circ$F))
l	over-all length of flow passage, (ft)
P_w	wetted perimeter, (ft)
Pr	Prandtl number, $c_p\mu/k$
Δp	static pressure drop, (lb/sq ft)

s	transverse wall-to-wall spacing between fins in same row, (in.), (fig. 1)
v	fluid velocity, (ft/sec)
δ	thickness of fin metal, (in.), (fig. 1)
λ	length of fin in direction of fluid flow (ft except where specified as in.), (fig. 1)
μ	absolute fluid viscosity, (lb/(sec)(ft))
ρ	weight density, (lb/cu ft)
σ	transverse stagger spacing between fins in successive rows, (in.), (fig. 1)

RESULTS AND DISCUSSION

From consideration of the variables that may be of importance in the heat-transfer and friction processes occurring in staggered-fin passages (fig. 1), the following functional relations were assumed:

$$\left(\frac{h}{c_p G}\right) Pr^{2/3} = F_1\left(\frac{Gd_h}{\mu}, \frac{\lambda}{d_h}, \frac{\delta}{s}, \frac{\sigma}{s}\right)$$

$$f = F_2\left(\frac{Gd_h}{\mu}, \frac{\lambda}{d_h}, \frac{\delta}{s}, \frac{\sigma}{s}\right)$$

The ranges of the indicated dimensionless groupings covered in references 1 to 5 are shown in the table of figure 1. The data of these references were examined in terms of the indicated dimensionless groupings and correlation of the data was made on the basis of the groupings found to be important in the range of conditions covered by the experiments.

Plots of the heat-transfer and friction data of reference 1 obtained for the staggered-fin-passage arrangement over a fairly wide range of values of Reynolds number Gd_h/μ are presented in figure 2. In figure 2(a), the heat-transfer grouping $(h/c_pG)Pr^{2/3}$ is plotted against Gd_h/μ; in figure 2(b), the friction factor f

is plotted against Gd_h/μ. A single line is drawn in figure 2(a) that fits the heat-transfer data well over the range of Gd_h/μ from 370 to 9020. Although a transition from laminar to turbulent boundary layer very probably occurs in this range of Gd_h/μ, such transition produces no noticeable effect on heat transfer. In figure 2(b), however, adequate representation of the friction data requires the use of two separate lines: one line is applicable for values of Gd_h/μ less than about 3500 and the other line is applicable for values of Gd_h/μ greater than about 3500. The necessity for separate correlation lines for the friction data for values of Gd_h/μ above and below about 3500 probably results from a transition from laminar to turbulent boundary layer.

Plots of the heat-transfer and friction data of reference 2 are presented in figure 3, wherein a systematic variation of the parameter λ/d_h is made to ascertain its effect on heat transfer and friction. In figure 3(a), $(h/c_pG)Pr^{2/3}$ is plotted against Gd_h/μ for values of λ/d_h of 0.90, 2.25, 4.50, and 9.0; in figure 3(b), f is plotted against Gd_h/μ for the same values of λ/d_h. As shown in figure 3(a), the variation of λ/d_h does not alter the conclusion drawn from figure 2(a) that for any one value of λ/d_h a single line represents the heat-transfer data over the entire range of Gd_h/μ investigated; figure 3(b) also confirms the conclusion that for each value of λ/d_h the friction data undergo a transition at a value of Gd_h/μ of about 3500.

Figure 3 shows that in the low range of λ/d_h values, both $(h/c_pG)Pr^{2/3}$ and f rapidly decrease with increase in λ/d_h. At the high λ/d_h values, however, both $(h/c_pG)Pr^{2/3}$ and f are relatively insensitive to changes in λ/d_h. This insensitivity at the high λ/d_h values is to be expected because as λ/d_h becomes larger the boundary layer approaches full development before interruption and the undeveloped portion of the boundary layer contributes a small share to the over-all heat-transfer and friction processes.

For convenience of correlation and presentation of data, λ/d_h can be assigned a critical value, herein denoted as $(\lambda/d_h)_c$, above which the variation in λ/d_h produces negligible effect on $(h/c_pG)Pr^{2/3}$ and f. Below this assigned value of $(\lambda/d_h)_c$, the

effect of λ/d_h on $(h/c_pG)Pr^{2/3}$ and f must be accounted for. The value of $(\lambda/d_h)_c$ can be estimated from figure 3, but the actual choice of $(\lambda/d_h)_c$ was made herein on the basis of correlation of all the data currently available (references 1 to 5) and will be subsequently discussed.

The effects of δ/s and σ/s cannot be examined independently of the other variables because systematic variations of δ/s and σ/s are not reported in references 1 to 5. The data of the reference reports, however, cover the range of σ/s and δ/s of interest in interrupted-fin exchangers, hence, a correlation of all these data would reveal whether there are any important trends in the heat transfer and friction due to these variables over the range of interest. The effects of δ/s and σ/s will be examined on this basis.

The final results of a detailed study of various bases for correlating all the available data are presented in figures 4 and 5. The best correlation of the data was obtained for a value of $(\lambda/d_h)_c$ equal to 3.5; hence, in figures 4 and 5, the variation of λ/d_h is explicitly accounted for when λ/d_h is less than or equal to 3.5 and is taken to produce no additional effect on heat transfer and friction as λ/d_h increases beyond 3.5.

In figure 4, $(h/c_pG)Pr^{2/3}$ is plotted against $\sqrt{(\lambda/d_h)(Gd_h/\mu)}$ for λ/d_h less than or equal to 3.5; for λ/d_h greater than 3.5, the abscissa in figure 4 becomes $\sqrt{3.5(Gd_h/\mu)}$. The data plotted are those presented in references 1 to 3 and 5; the heat-transfer data of reference 4 were in a form that could not be converted to $(h/c_pG)Pr^{2/3}$. A single line satisfactorily correlates all the data; all but two of the points are within ±20 percent of the line and the bulk of the data is well within these limits.

The data correlated in figure 4 cover a range of δ/s from about 0.04 to 0.25 (δ varies from 0.005 to 0.10 in.) and σ/s from about 0.18 to 0.50. The good data correlation in figure 4 thus indicates that δ/s and σ/s are unimportant variables affecting heat transfer in staggered fin passages over the ranges covered. The equation of the line through the data is

$$\left(\frac{h}{c_p G}\right)Pr^{2/3} = \frac{0.60}{\sqrt{\left(\frac{\lambda}{d_h}\right)\left(\frac{Gd_h}{\mu}\right)}} \qquad \text{for } \lambda/d_h \leq 3.5$$

and becomes

$$\left(\frac{h}{c_p G}\right)Pr^{2/3} = \frac{0.60}{\sqrt{3.5\left(\frac{Gd_h}{\mu}\right)}} \qquad \text{for } \lambda/d_h > 3.5$$

In figure 5(a), which is for values of Gd_h/μ up to 3500, f is plotted against $(\lambda/d_h)(Gd_h/\mu)^{0.67}$ for λ/d_h less than or equal to 3.5; for λ/d_h greater than 3.5, the abscissa in figure 5(a) becomes $3.5(Gd_h/\mu)^{0.67}$. The data plotted in figure 5(a), which is for Gd_h/μ less than or equal to 3500, are those reported in references 1 to 3 and 5; all the data of reference 4 were obtained for Gd_h/μ greater than 3500.

In figure 5(a), 90 percent of the friction data of references 2, 3, and 5 can be represented within ±15 percent by a single line; the data for the thick fins of reference 5 lie slightly above the data for the much thinner fins of the other references. The data of reference 1 fall parallel to but much lower than the data of the other references. The discrepancy cannot be due to the exponents of λ/d_h and Gd_h/μ because the parallelism of all the data on logarithmic coordinates shows that the exponents have been correctly determined. The discrepancy is not due to the effects of δ/s or σ/s because reference 3, which reports δ/s and σ/s values that fall within the range of the values of reference 1, agrees well with the remaining references. The reason for the discrepancy is not definitely known but it is interesting to note that the discrepancy disappears if the λ/d_h values reported for friction in reference 1 are multiplied by a factor of 2. The equation for the data of references 2, 3, and 5 given in figure 5(a) for Reynolds numbers up to 3500 is

$$f = \frac{11.8}{\left(\frac{\lambda}{d_h}\right)\left(\frac{Gd_h}{\mu}\right)^{0.67}} \qquad \text{for } \lambda/d_h \leq 3.5$$

and becomes

$$f = \frac{11.8}{3.5\left(\frac{Gd_h}{\mu}\right)^{0.67}} \qquad \text{for } \lambda/d_h > 3.5$$

Figure 5(b), which is presented for Gd_h/μ greater than 3500, is a plot of f against $(\lambda/d_h)(Gd_h/\mu)^{0.24}$ for λ/d_h less than or equal to 3.5. For λ/d_h greater than 3.5, the abscissa in figure 5(b) becomes $3.5(Gd_h/\mu)^{0.24}$. The data plotted are taken from references 1 to 5. As indicated in this figure, 87 percent of the friction data of references 2 to 5 can be correlated within ±20 percent by a single line. The friction data of reference 1 fall considerably lower than the data of the remaining references, as was also shown in figure 5(a). No reason for this discrepancy is known; however, it is of interest to note that the discrepancy disappears if the λ/d_h values reported for friction in reference 1 are multiplied by 2.

The friction data correlated in figure 5 cover a range of σ/s from about 0.18 to 0.50. Examination of the correlations indicates that any effect of σ/s on f that may be present is hidden by the scatter of the data; hence, in the range indicated, σ/s is an unimportant variable affecting friction in staggered plane fin passages.

The data of references 2 to 5 that satisfactorily correlated in figure 5 cover a wide enough range of δ/s (from about 0.07 to 0.25) to indicate that the effect of δ/s on f over this range is of the same order of magnitude as the data scatter. A satisfactory approximation of the friction factor is thus obtainable without explicit accounting for fin thickness although there appears to be a slight trend of increasing f with δ/s.

The equation of the line through the bulk of the data of references 2 to 5 for Reynolds numbers greater than 3500 is

$$f = \frac{0.38}{\left(\frac{\lambda}{d_h}\right)\left(\frac{Gd_h}{\mu}\right)^{0.24}} \qquad \text{for } \lambda/d_h \leq 3.5$$

and

$$f = \frac{0.38}{3.5\left(\frac{Gd_h}{\mu}\right)^{0.24}} \qquad \text{for } \lambda/d_h > 3.5$$

At the transition value, Gd_h/μ equal to 3500, the equations for the lines of figure 5 give friction factors that are in the ratio $(0.38/11.8)(3500)^{0.43}$, which is equal to 1.08.

SUMMARY OF RESULTS

A study of the experimental data available from five reference reports on the heat-transfer coefficients and friction factors of fluids flowing past interrupted plane fins staggered in successive rows in the direction of fluid flow showed that

1. The principal parameters governing the heat-transfer coefficient and the friction factor are the Reynolds number based on fin-passage hydraulic diameter and the ratio of fin length to fin-passage hydraulic diameter. The friction factor moderately increased for large increases in the ratio of fin thickness to fin transverse spacing but a good estimate of the friction factor was obtained without considering fin thickness. Any effects that were produced by the stagger arrangement of successive rows were not detectable within the scatter of the available data.

2. The heat-transfer coefficient and the friction factor became insensitive to the ratio of fin length to fin-passage hydraulic diameter for values of the ratio above 3.5.

3. Correlation equations were obtained for the heat-transfer data and for the friction data. A single equation represented the available heat-transfer data over the entire range of conditions investigated. The friction data required separate correlation equations below and above the transition Reynolds number of 3500.

Lewis Flight Propulsion Laboratory,
National Advisory Committee for Aeronautics,
Cleveland, Ohio, August 13, 1950.

REFERENCES

1. Norris, R. H., and Spofford, W. A.: High-Performance Fins for Heat Transfer. Trans. A.S.M.E., vol. 64, no. 5, July 1942, pp. 489-496.

2. Joyner, Upshur T.: Experimental Investigation of Entrance-Region Heat-Transfer Coefficients. NACA ARR 3K01, 1943.

3. London, A. L., and Ferguson, C. K.: Gas Turbine Plant Regenerator Surfaces - Basic Heat Transfer & Flow Friction Data. Res. Memo. No. 2-46, Bur. Ships, Navy Dept., July 1, 1946. (Navships (250-338-3).)

4. Küchemann, D., and Weber, J.: 2. The Processes of the Flow. 2.1. The Radiator in the Straight Duct. AVA Monographs, Reps. and Trans. No. 915, British M.A.P., Sept. 1, 1947.

5. Kays, W. M.: The Performance of Finned-Flat-Tube Heat Exchanger Surfaces. Tech. Rep. No. 6, Dept. Mech. Eng., Stanford Univ., Aug. 15, 1949. (Navy Contract N6-ONR-251, T.O. 6.)

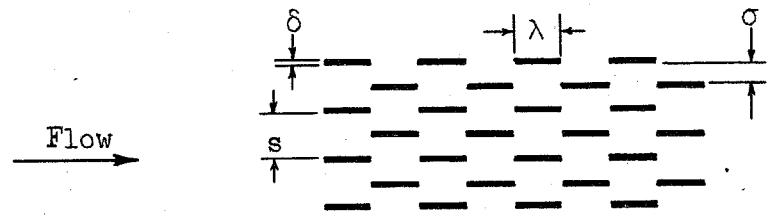

Reference	Sample	λ (in.)	s (in.)	δ (in.)	σ (in.)	d_h (in.)	λ/d_h	δ/s	σ/s	Gd_h/μ
1	1	0.125	0.115	0.010	0.0383	0.206	0.606	0.087	0.33	380 - 9020
	2		.120	.005	.040	.200	.625	.042	.33	370 - 8460
	10		.115	.010	.0575	.206	.606	.087	.50	480 - 6110
2	--	0.20	0.125	0.0313	0.0625	0.222	0.90	0.248	0.50	1600 - 15,000
	--	.50					2.25			1600 - 17,750
	--	1.0					4.50			1000 - 10,350
	--	2.0					9.0			1000 - 20,000
3	J	0.250	0.084	0.006	0.035	0.121	2.07	0.071	0.42	420 - 7720
4	h	0.197	0.0878	0.0118	0.0439	0.142	1.39	0.134	0.50	4000 - 20,000
	g	.859	.0878	.0118	.0439	.146	5.89	.134		4800 - 15,000
	e	.406	.164	.0083	.082	.252	1.61	.051		6600 - 32,000
5	9.1-.737-S	0.737	0.45	0.100	0.08	0.166	4.44	0.222	0.178	490 - 9260

Figure 1. - Schematic diagram of interrupted plane fins staggered in successive rows and ranges of fin parameters of reference reports.

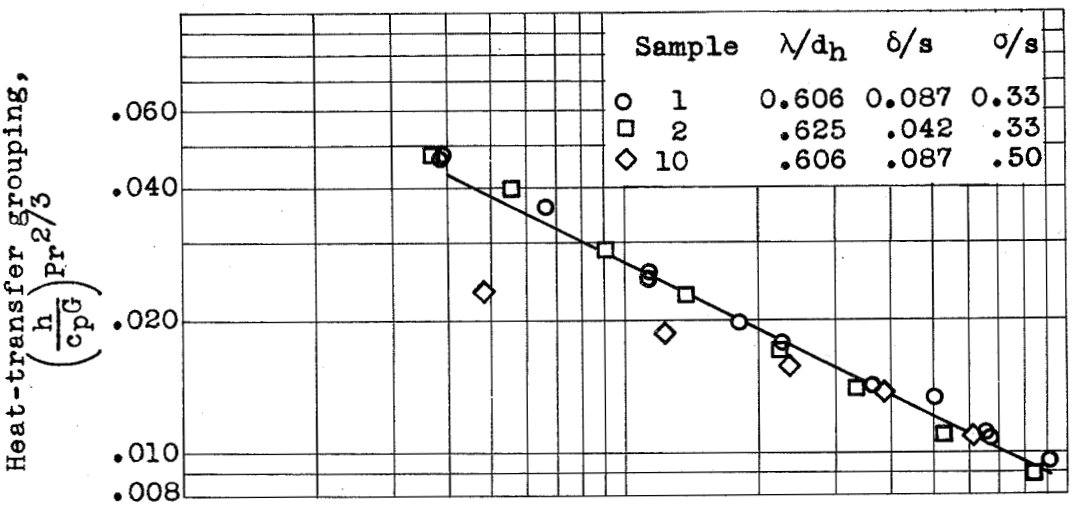

(a) Variation of heat-transfer grouping with Reynolds number.

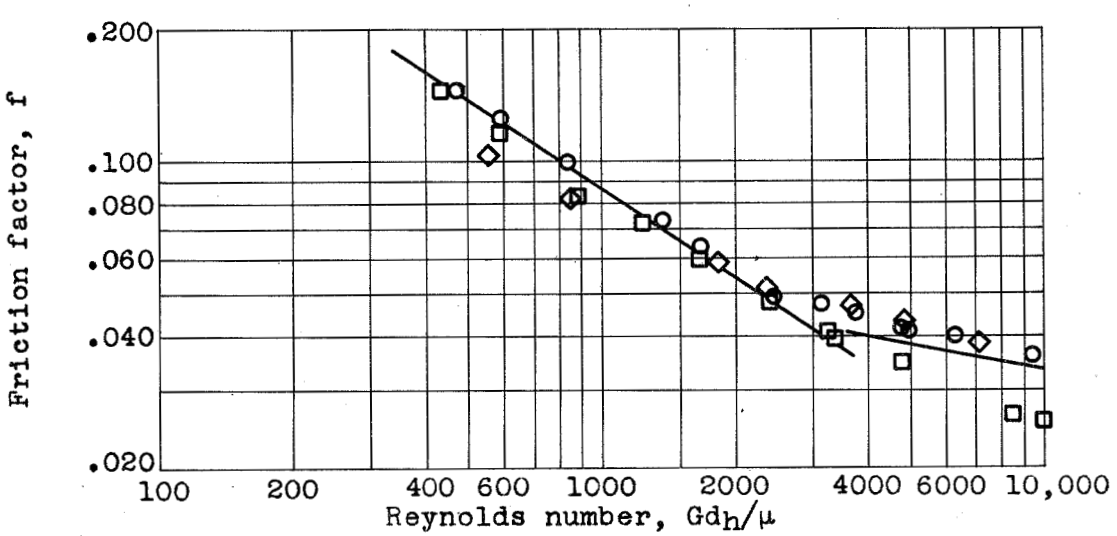

(b) Variation of friction factor with Reynolds number.

Figure 2. - Variation of heat-transfer and friction parameters with Reynolds number for essentially constant λ/d_h. (Data are taken from reference 1.)

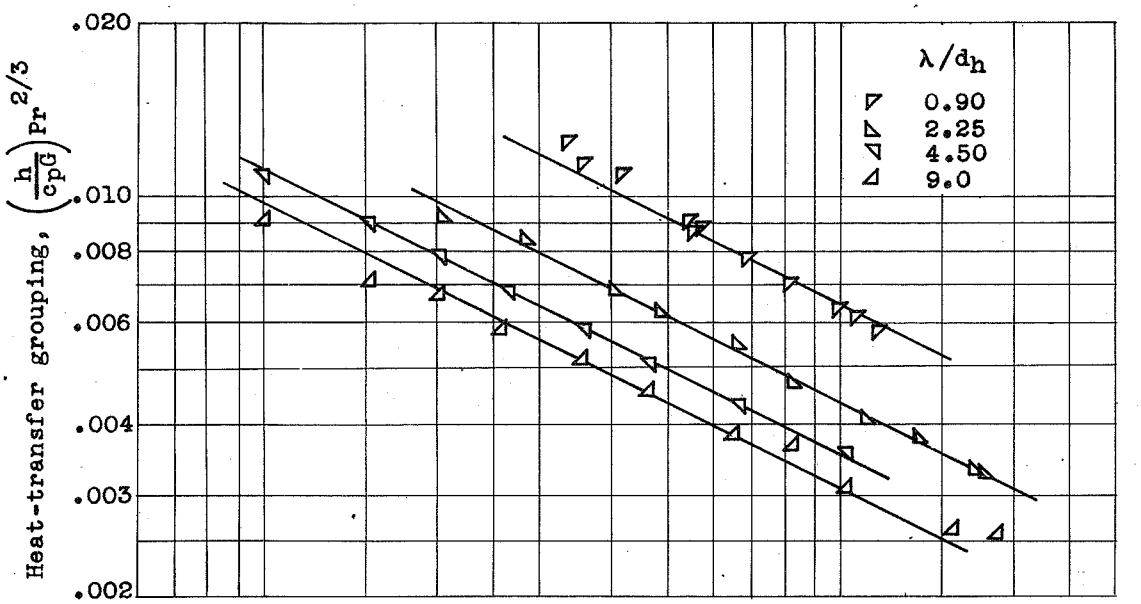

(a) Variation of heat-transfer grouping with Reynolds number.

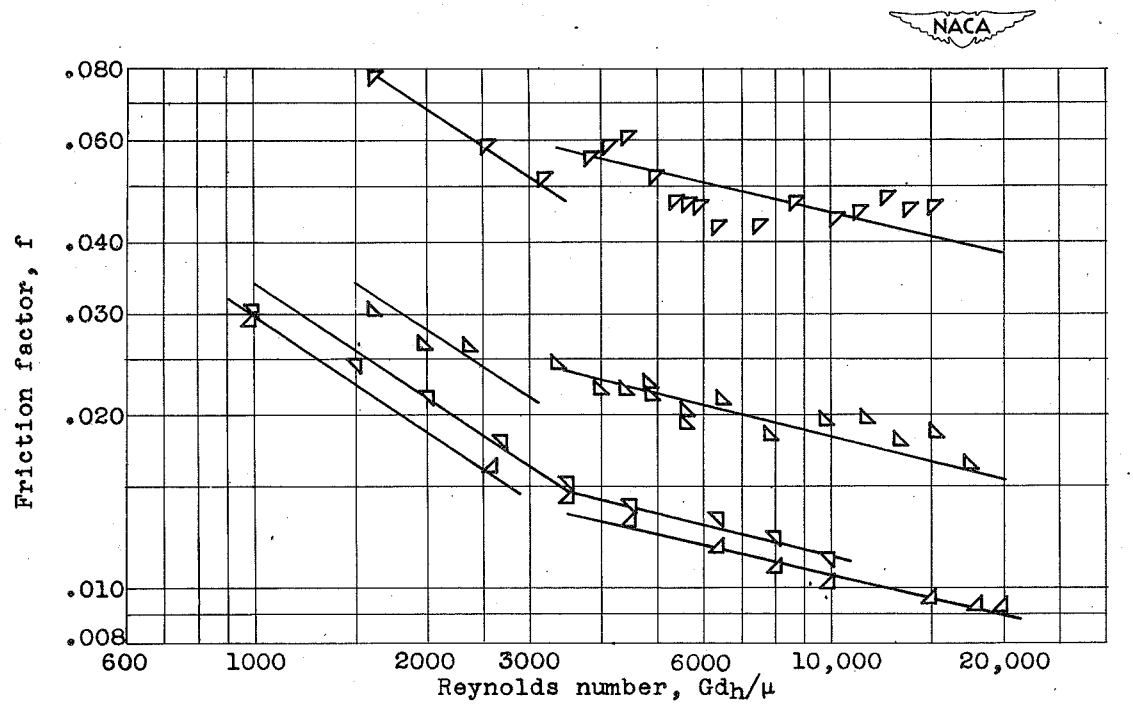

(b) Variation of friction factor with Reynolds number.

Figure 3. - Variation of heat-transfer and friction parameters with Reynolds number for various values of λ/d_h and for δ/s of 0.248 and σ/s of 0.50. (Data are taken from reference 2.)

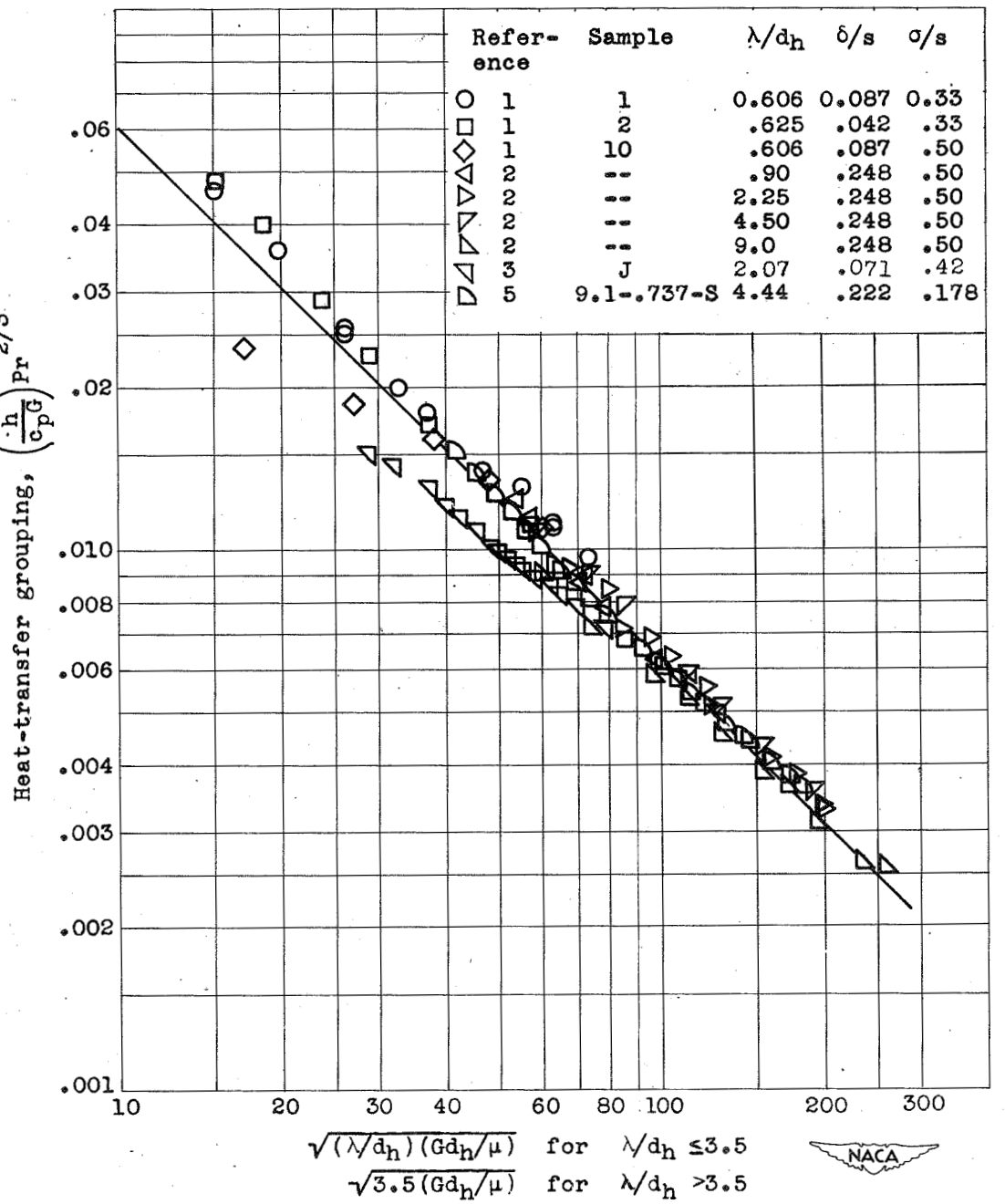

Figure 4. - Variation of heat-transfer grouping with $\sqrt{(\lambda/d_h)(Gd_h/\mu)}$ for values of λ/d_h less than or equal to 3.5 or with $\sqrt{3.5(Gd_h/\mu)}$ for values of λ/d_h greater than 3.5.

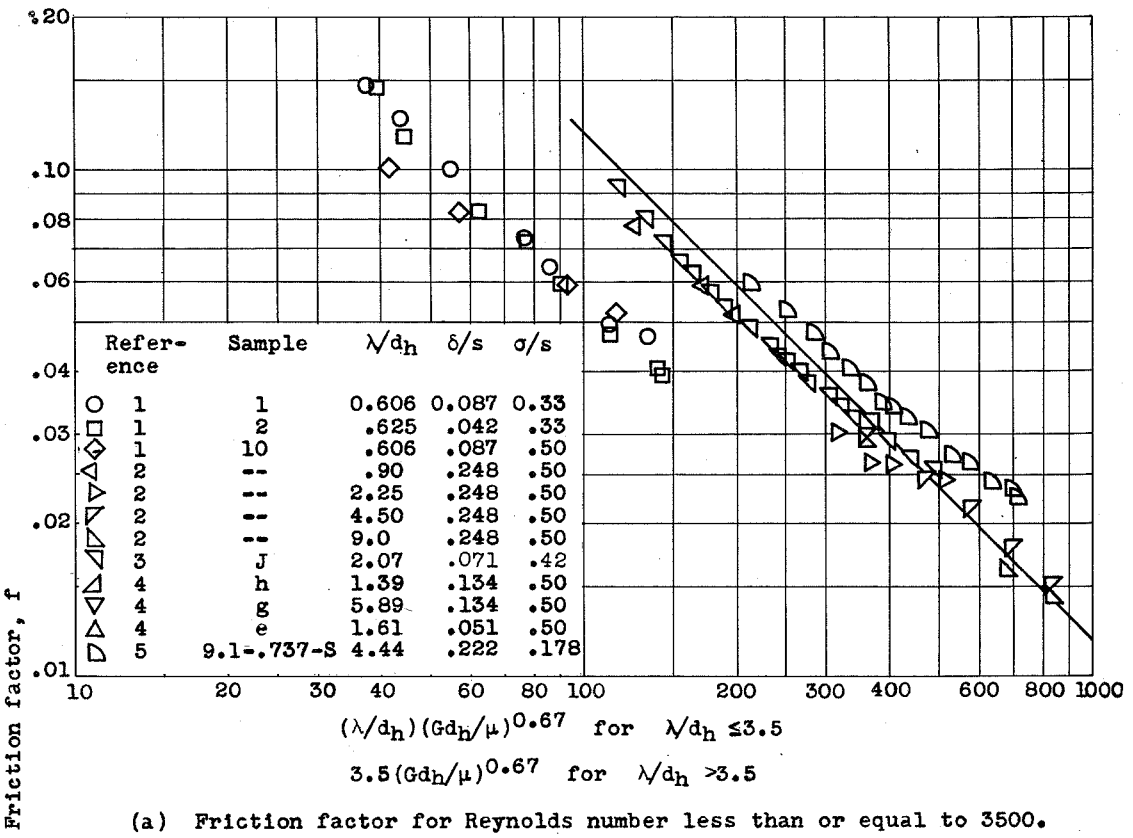

Reference		Sample	λ/d_h	δ/s	σ/s
○	1	1	0.606	0.087	0.33
□	1	2	.625	.042	.33
◇	1	10	.606	.087	.50
△	2	--	.90	.248	.50
▷	2	--	2.25	.248	.50
▽	2	--	4.50	.248	.50
◁	2	--	9.0	.248	.50
◁	3	J	2.07	.071	.42
△	4	h	1.39	.134	.50
▽	4	g	5.89	.134	.50
△	4	e	1.61	.051	.50
▷	5	9.1-.737-S	4.44	.222	.178

(a) Friction factor for Reynolds number less than or equal to 3500.

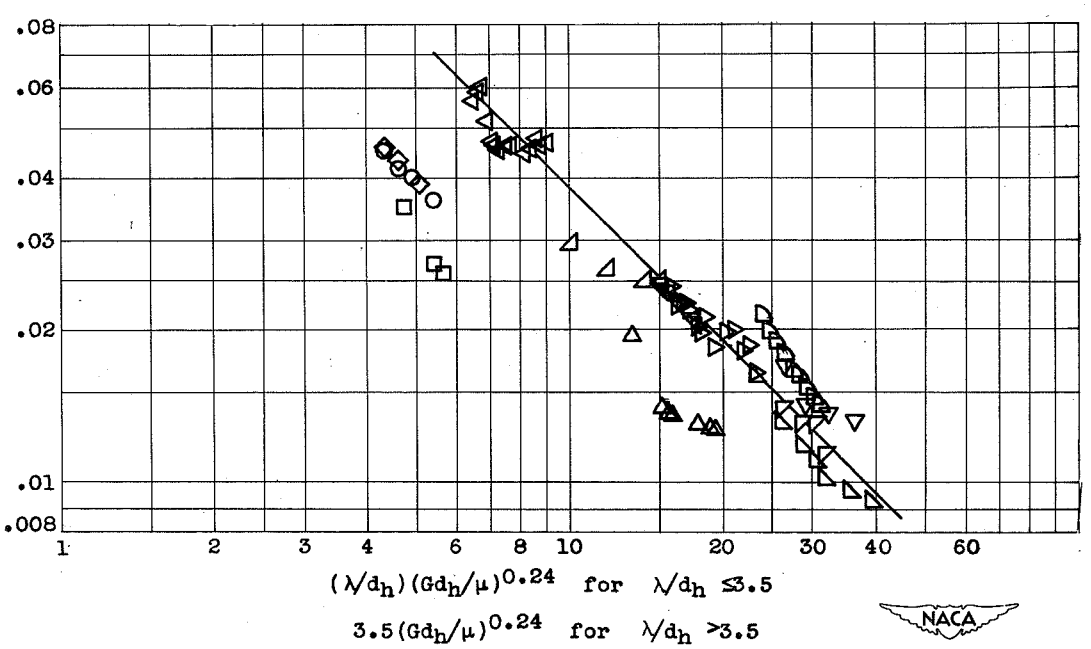

(b) Friction factor for Reynolds number greater than 3500.

Figure 5. - Variation of friction factor with pertinent dimensionless parameters above and below transition Reynolds number of 3500.